Rotational Tunnelling in Binary Tetramethylmetal Mixtures

Michael Prager[a], Da Zhang[b], and Al. Weiss[b]

[a] Institut für Festkörperforschung der KFA Jülich, Postfach 19 13, D-52428 Jülich, Germany
[b] Institut für Physikalische Chemie III der Technischen Hochschule, Petersenstr. 20, D-64287 Darmstadt, Germany

Z. Naturforsch. **50a**, 405–412 (1995); received December 15, 1994

Dedicated to Professor Müller-Warmuth on the occasion of his 65th birthday

Mixed $Pb_cSn_{1-c}(CH_3)_4$ samples with $c = 0.0, 0.1, 0.2, 0.25, 0.48, 0.5, 0.75, 0.85$, and 1.0 and mixed $[Pb(CH_3)_4]_c[Sn(CD_3)_4]_{1-c}$ samples with $c = 0.02$ and 0.09 were investigated by high resolution inelastic neutron scattering. Rotational tunnelling transitions are observed for energy transfers $\hbar\omega < 100$ μeV. The global features are interpreted in a single particle model. A strong matrix effect of the Pb component is attributed to changes of potential symmetry. Effects beyond the expectation of the single particle description are found.

1. Introduction

The tetramethylmetal compounds form an interesting class of materials where the individual molecules in the lattice are bound together via the shell of methyl tunnel rotors [1–3]. The methyl rotational potentials are weak and the quantum tunnel splittings are accessible to high resolution inelastic neutron spectroscopy. Despites the obvious need of intermolecular interactions in forming a solid, first NMR experiments were interpreted under the assumption of purely intramolecular potentials. This view was based on the systematic increase of the tunnel splitting with the size of the molecule or the correlated intramolecular methyl-methyl distances [2]. Later the relative importance of intra- and intermolecular interaction was estimated from a comparison of spectra obtained from the pure material [4] and individual molecules isolated in an argon matrix [5]. These data clearly show that both forces are of similar magnitude. The recently refined crystal structure [6] confirms this view. The arrangement in the solid reduces the symmetry of the free molecule $\bar{4}3m$ toward a 3-fold axis at the molecular site in the Pa3 crystal structure. The strong intermolecular interaction is accompanied by a significant distortion of the molecules along one 3-fold axis in the crystal field of reduced symmetry. The inequivalency of methyl groups leads to a spectrum consisting of two sets of tunnelling transitions with relative intensities 3:1 as required by the occurrence probabilities of the two CH_3 sites. The pure materials show tunnel transitions at 30.7 and 74 μeV for tetramethyllead (TML) and 13.2 and 1.72 μeV for tetramethyltin (TMT), respectively. The first mentioned transitions show the stronger intensities. On the basis of the qualitative similarity of the tunnelling spectra it can be assumed that TMT has the same low temperature crystal structure Pa3 as TMT. The lattice parameters of the two constituents of about 11 Å differ very little (10^{-3}) with the larger molecule TML showing the smaller unit cell [7]. In consistence with the crystal structure, the NMR-T_1 spin lattice relaxation curves represent the superposition of two processes related with the two species of methyl groups present in these materials [1, 4, 8].

Deuteration of the environment increases the rotational potential of the protonated species h-TMT [9]. Due to the different molecular sizes TML is believed to cause much stronger local distortion than a deuterated methyl group in TMT. In mixed TML/TMT methyl tunnelling frequencies of both molecules are in the range of neutron spectrometers. This allows to study the mutual influences simultaneously.

It was shown in a previous conference contribution that in case of TMT/TML mixtures the tunnelling spectra follow qualitatively the lines expected from the single particle rotation model of rotational tunnelling [10]. The present paper wants to extend this view and also concentrates on more delicate questions as the effect of deuterating one species. In case of h-TMT/d-TMT mixtures it was found that well defined subspecies, probably related with the character of the next neighbour molecule, h or d, appeared [9]. Finally the possible influence of direct methyl-methyl coupling will be considered.

Reprint requests to Dr. M. Prager.

0932-0784 / 95 / 0400-0405 $ 06.00 © – Verlag der Zeitschrift für Naturforschung, D-72027 Tübingen

2. Experimental and Results

H-TMT of purity 99% was obtained from Aldrich and used without further purification. The deuterated molecule was prepared according to literature [3]. Pure TML was prepared from commercially available TML/toluene mixtures in a complex sequence of chemical reactions [3]. Binary mixtures of TMT/TML were prepared by adding the liquid components in the wanted volume ratio together. The samples were filled into aluminum sample containers, sealed and cooled down in a liquid helium cryostat to $T = 2-5$ K.

High resolution neutron scattering data were taken at two different spectrometers of the ILL, Grenoble. The TMT/TML were studied at high energy transfers up to 100 μeV using the time of flight spectrometer IN5 with an incoming wavelength $\lambda = 13$ Å ($\delta E = 6.6$ μeV FWHM). The low energy transfer range of this system was studied using the backscattering spectrometer IN10 in its standard, its CaF_2 [111] offset configuration and with the new KCl temperature monochromator [11].

Figure 1 shows an overview on the concentration dependence of the tunnelling spectra as obtained on IN5. Figures 2 and 3 show the spectra of TML/TMT at TML concentrations $c = 0.85$ and $c = 0.15$, respectively. The spectra in each figure with the larger number of tunnelling peaks are obtained from the fully protonated systems while the spectra with fewer inelastic peaks reproduce the results of h-TML in d-TMT. The solid lines represent fits with gaussians for every inelastic line. The intensity ratios of tunnelling transitions belonging to the same molecule were kept constant according to the occurrence probability of the respective type of methyl groups. The position, width and relative intensity of the TML and TMT subsystem were free parameters of the fit. The fit results are graphically represented in Figure 4.

Figure 5 represents spectra of TML/TMT mixtures at large TML concentrations $c = 0.95$ and $c = 0.85$. Due to the better energy resolution of the IN10 backscattering spectrometer in its CaF_2 offset configuration the tunnel lines from TMT and TML, respectively, are now well resolved and its relative intensities can be better determined. For low TML concentrations $c = 0.02$ and $c = 0.09$ and a d-TMT environment similar spectra are shown in Figure 6.

For the same range of TML concentrations, $c = 0.1$ and $c = 0.2$, the regime of the lowest energy transfers

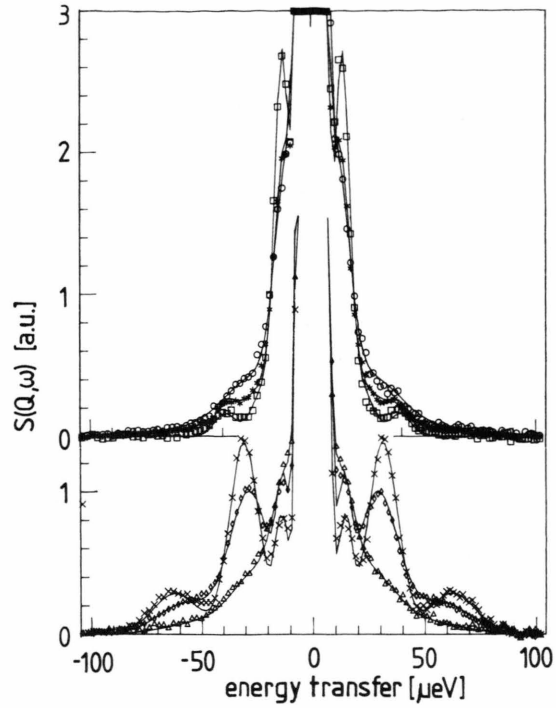

Fig. 1. Tunnel spectra of $Pb_cSn_{1-c}(CH_3)_4$, $c = 0.85$ (×), 0,75 (◇), 0.5 (△), 0.37 (○), 0.25 (*), 0.1 (□). Samples temperature $T_S = 2$ K. *Spectrometer:* IN5 of the ILL, $\lambda_i = 13$ Å. $\delta E = 6.6$ μeV (FWHM). The solid lines are fits with gaussians of correlated intensities (see the text).

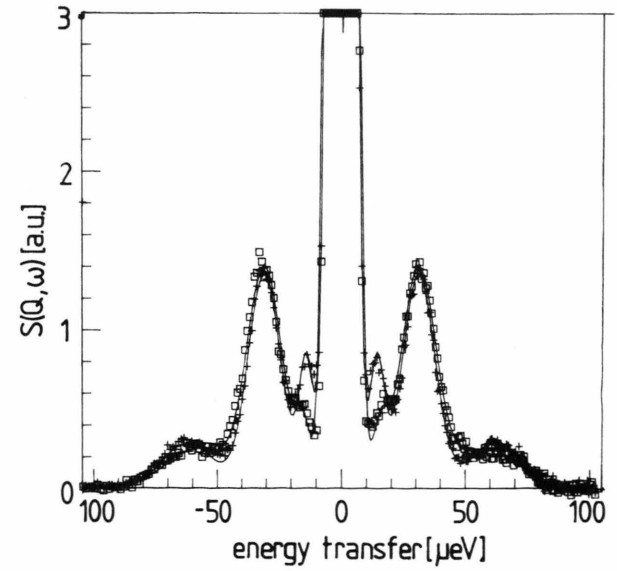

Fig. 2. Tunnel spectra of $[Pb(CH_3)_4]_{0.85}[Sn(CX_3)_4]_{0.15}$, $X = H$ (+), $X = D$ (□). Other parameters like in Figure 1.

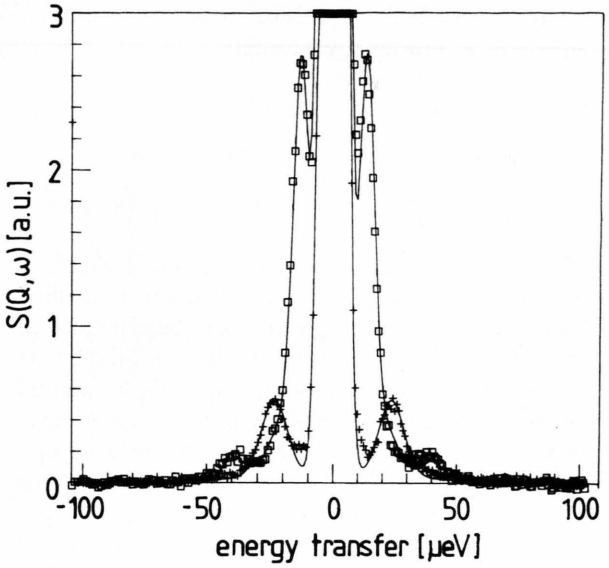

Fig. 3. Tunnel spectra $[Pb(CH_3)_4]_{0.10}[Sn(CX_3)_4]_{0.90}$, $X = D$ (+), $X = H$ (□). Other parameters like in Figure 1.

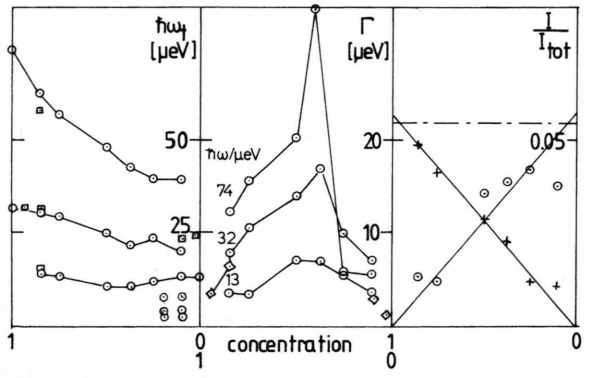

Fig. 4. Dependence of tunnel frequencies $\hbar\omega_t$, linewidths Γ of the main lines, and relative intensities I/I_{tot} of TML/TMT on the concentration of TML as derived from the spectra of Fig. 1 and similar ones. Squares correspond to samples of protonated TML in deuterated TMT.

was measured on IN10 in its classical Doppler set-up with polished Si[111] analysers (Figure 7) and in the newly established temperature scan mode (Figure 8). This latter mode has the advantage to cover a wider energy range with about the same energy resolution. In our case this allows to study all tunnel transitions in one spectrum. For reasons of better statistics the spectrum is compressed in the range of larger energy transfers and shown as inset. The most astonishing

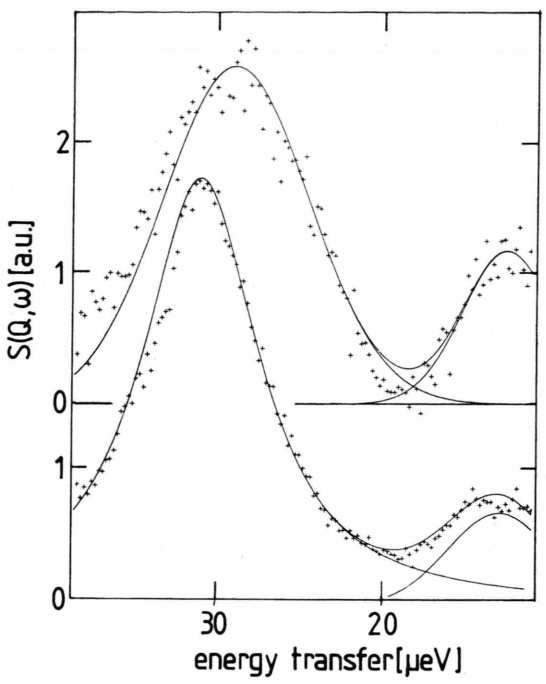

Fig. 5. Tunnel spectra of $[Pb(CH_3)_4]_c[Sn(CH_3)_4]_{1-c}$, $c = 0.85$ (top), $c = 0.95$ (bottom). Other parameters like in Figure 1.

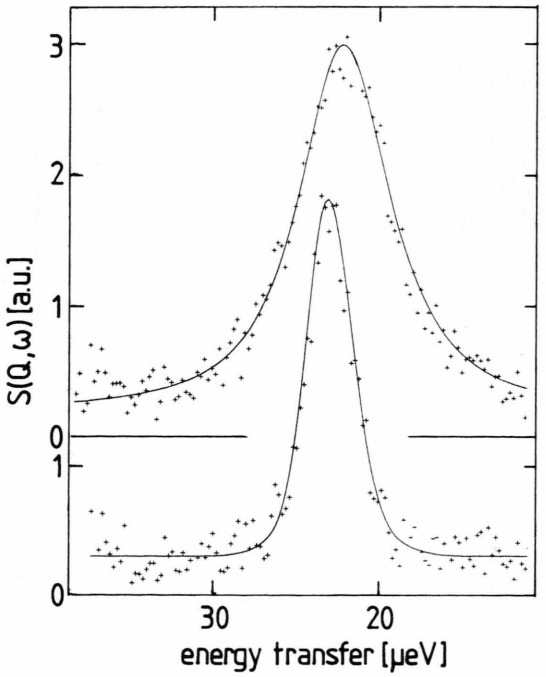

Fig. 6. Tunnel spectra of $[Pb(CH_3)_4]_c[Sn(CD_3)_4]_{1-c}$, $c = 0.09$ (top), $c = 0.02$ (bottom). Other parameters like in Figure 1.

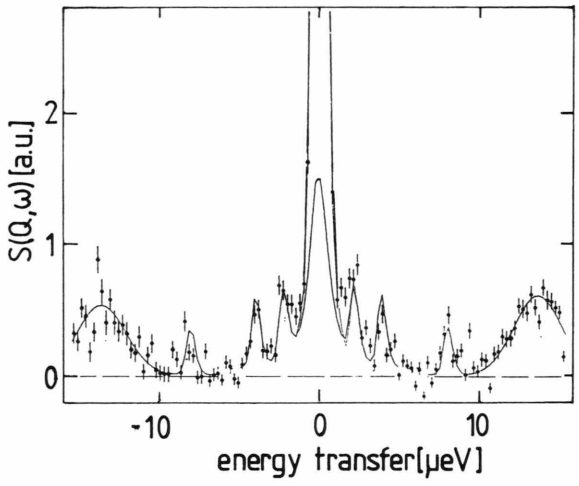

Fig. 7. Tunnel spectrum of $[Pb(CH_3)_4]_{0.20}[Sn(CH_3)_4]_{0.80}$. Sample temperature $T_S = 4$ K. *Spectrometer:* IN10 of the ILL, polished Si(111) monochromator and analysers, $\delta E = 0.4$ μeV (FWHM).

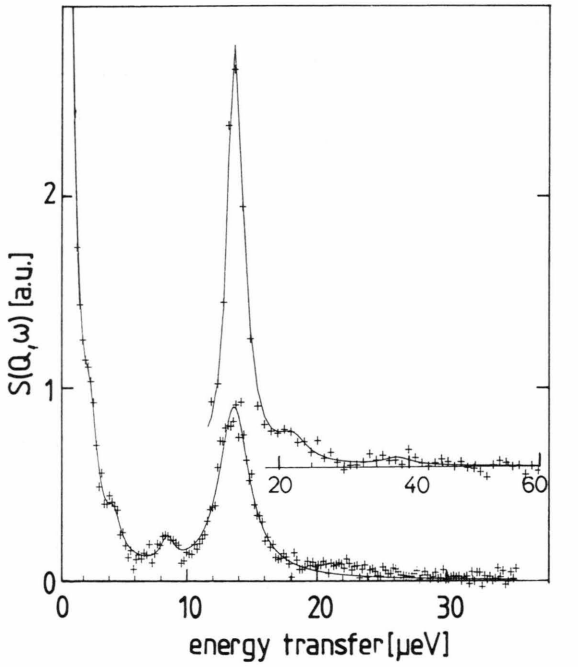

Fig. 8. Tunnel spectrum of $[Pb(CH_3)_4]_{0.10}[Sn(CH_3)_4]_{0.90}$. Sample temperature $T_S = 4$ K. *Spectrometer:* IN10 of the ILL, temperature variable KCl monochromator, unpolished Si(111) analysers, $\delta E \sim 2.0$ μeV (FWHM). *Inset:* Compressed presentation of the high energy transfer range.

feature is here the appearance of new well defined excitations at low energy transfers.

3. Discussion

3.1. Single Particle Description

The results of all fits are shown together in Figure 4. The global changes of the low resolution tunnelling spectra with sample composition can be explained in a model of single particle rotation. In such a model the main effect of an impurity is to rescale the rotational potential of neighboring molecules. Such models have been successfully used to describe methane in rare gases [12] or mixed protonated/deuterated methane [13]. Beside of very small concentrations of one component where individual surroundings are occasionally distinguishable [12] this model usually predicts smooth changes of the spectra. In a system containing inequivalent rotors it is expected that the number of distinguishable tunnel rotors remains the same at all concentrations, their weights being given by the occurrence probabilities $p(n)$ of the species and the concentration c. The possibility of distinguishable surroundings is discussed in Section 3.5.

With energy resolution of IN5 smooth changes of tunnelling energies are found over the whole concentration range (Fig. 4, left). The derived parameters are rather unique at low concentrations of each constituent, $c \leq 0.25$ and $c \geq 0.75$. This is not the case for intermediate concentrations.

Statistically mixed binary systems show a maximum of disorder at equal concentration of both components. In agreement with this prediction the widths of TML lines explode around $c = 0.4$ and the spectra loose part of their structure. Such smooth scattering functions might be described various different ways. Thus, while the data description at low and high concentrations is free of arbitrary assumptions the extraction of parameters at intermediate concentrations is depending on the applied model. We have forced the analysis to follow the expectation of the single particle model. Intensities are taken proportional to site probability $p(n)$ and concentration, $I \sim p(n) \cdot c$, in this regime (Fig. 4, center).

To relate the intensities from different samples and to compare with theoretical models the intensities are shown relative to the total scattering, which is the sum of the elastic line and all tunnelling transitions. By this

method one can avoid an absolute calibration of the spectrometer. One only obtains reliable numbers, however, if the elastic scattering is not contaminated. It is the advantage of the long wavelength $\lambda = 13$ Å used that no Bragg reflections can be excited in our systems (lattice parameter ~ 11.2 Å and Pa3 space group [6]). Corresponding theoretical values are determined from the single particle scattering function using tunnelling structure factors [14] at the experimental momentum transfer $\bar{Q} = 0.81$ Å^{-1}. We know that the low energy tunnelling line of TMT at $\hbar\omega_t \sim 1.8$ μeV contributes to the elastic line at the experimental energy resolution. Taking this into account, we get the relative inelastic intensity as the dashed line in Fig. 4, right in complete agreement with the experimental data. To obtain a quantitatively good fit it was necessary, however, to allow the relative intensities of the two constituents to deviate from their concentration ratio. While the TML intensity follows almost exactly the expected linear increase with concentration, the TMT values scatter significantly (Figure 4, right). In the case of IN5 spectra (Fig. 1) this result might be excusable by the overlap with the elastic line. The well resolved spectra of Fig. 5, however, similarly show an enhanced TMT intensity. The corresponding points in Fig. 4, right are obtained by arbitrarily fixing the intensity of the TML transition to the value expected from theory.

3.2. *Matrix Effect*

The changes of characteristic molecular frequencies with environment are called matrix effect. The basis for comparison usually is the free molecule. Here we consider the changes compared to the pure compounds.

The 13 μeV line of TMT shows almost no shift if the molecule is incorporated in TML instead of TMT. At intermediate concentrations this splitting is somewhat reduced to 10.5 μeV. The line intensity at low TMT concentrations is to high. The line at 1.8 μeV becomes split into 3 lines in a TML environment. This observation cannot be explained as a matrix effect. We speculate about this observation in Section 3.5.

Contrary to TMT the CH_3 groups of TML show a very strong matrix effect. The transition at $\hbar\omega_t = 30.8$ μeV in pure TML shifts to $\hbar\omega_t \sim 22$ μeV in TMT. Similarly the transition at $\hbar\omega_t = 74$ μeV in pure TML is found at $\hbar\omega_t \sim 40$ μeV in TMT indicating significant changes either of potential strength or potential symmetry. This changes of the respective rotational potentials are discussed in more detail in Section 3.4.

3.3. *Isotope Matrix Effect*

The isotope matrix effect shall not be mixed up with the isotope effect which means the change of the tunnelling frequency of a methyl group with its deuteration. The isotope matrix effect describes the response of a system on the weakest form of chemical modification of an environment: its deuteration. Often it requires the sensitivity of rotational tunnelling to observe such an effect at all. Our spectra allow to document such isotope matrix effects for two concentrations.

1) For h-TML in h-TMT and d-TMT, respectively, and at $c_{Pb} = 0.1$ the tunnel splittings $\hbar\omega_h = (20\,(40)$ μeV shift to $\hbar\omega_d = 23$ μeV. No second tunnelling peak is found or resolved in the deuterated matrix. Relating the 20 μeV peak to the unique transition found in the d-TMT matrix a weak inverse isotope effect, i.e. a shift to larger tunnel splittings with deuteration, is confirmed.

2) For h-TML in h-TMT and d-TMT, respectively, and at $c_{Pb} = 0.85$ the tunnel splittings $\hbar\omega_h = 62\,(30.8)$ μeV shift to $\hbar\omega_d \sim 58\,(31.8)$ μeV. The values in parentheses show again an unusual inverse isotope effect.

3) For comparison the corresponding data for d-TMT in h-TMT are given. The tunnel splittings in pure h-TMT, $\hbar\omega_h = 13\,(1.72)$ μeV, shift to $\hbar\omega_d \sim 10\,(2.0)$ μeV in a deuterated environment [9]. Again one methyl group shows an inverse isotope matrix effect.

A qualitative understanding of the inverse isotope matrix effect can be based on the observation that in TML the more abundant methyl groups show the higher tunnel splitting while the situation is reverse in TMT. In the early publications [4, 8] this was taken as indication that the TML molecule is elongated, the TMT molecule compressed along the threefold axis of the site in the crystal. With this idea in mind it looks reasonable that in the TMT matrix the TML guest molecule is approaching the shape of the matrix molecules. This weakens the threefold axis of the crystal space group. The potentials and thus the tunnel splittings approach each other. Consequently the isotope effects are opposite in direction for the two species of methyl groups. This is also exactly what is observed in mixtures h-TMT/d-TMT [9]. For h-TML

in d-TMT it appears that the inequivalency of the methyl groups survives mainly in the linewidths. The tunnel frequencies of the TML methyl groups can no longer be distinguished.

3.4. Single Particle Rotational Potentials and Molecular Distortion

If we assume that the shape of the rotational potentials derived for the pure compounds [4, 8] do not change in the mixed system the reduction of the tunnel splitting from 30.8 (74) μeV in pure TML to 22 (40) μeV for TML in TMT must be due to an increase of the potential strenght. The potential is – as usual – described as

$$V(\varphi) = \sum_{n=1}^{2} \frac{V_{3n}}{2} \cdot (1 + (-1)^k \cos(3n\varphi)). \qquad (1)$$

The potential strength may be characterized by $VS = |V_3| + |V_6|$. Thus the observed shifts correspond to increases of potential strengths by 40% and 12% for the methyl groups on the threefold molecular axis ($\hbar\omega_t = 74$ μeV) and the more abundant species ($\hbar\omega_t = 30.7$ μeV), respectively (Table 1). The reduction of the relative difference of the two tunnelling transition energies would mean in this model that the molecular distortion is reduced in the TMT matrix compared to pure TML.

The changes of the strenghts of the rotational potentials guessed this way are incredibly large. This result cannot easily be reconciled with the observation that the pure systems TML and TMT show almost identical lattice parameters. Furthermore it looks strange that the TMT molecules do not show similarly strong shifts. – Rotational potentials represent the angle dependent part of the summed pair interactions. To get a different potential intermolecular distances should change. Under the restriction of almost equal lattice parameters this can happen only locally due to different interpenetration of TML with TMT molecules and might change more the symmetry than the strength of the rotational potential. Thus an alternative interpretation, more likely to us, assumes that the shape of the rotational potential changes with mixing. In such a model the reduced tunnel splitting is related to an increase of the threefold combined with a reduction of the sixfold term in the rotational potential. This tendency is expected from the description of the pure compounds and represents a further support of this explanation model. The low intensity tunnelling lines in TML and TMT are characterized by strong sixfold contributions V_6. The relative importance of V_6 is larger for TML (Table 1). It looks reasonable that the shape of the potential of a guest molecule develops toward the symmetry of the environment of its host lattice with decreasing concentration. – A change of just the potential symmetry is not able to explain the large matrix effect of the second TML tunnelling methyl group, however. A microscopic model to support the proposed model has to be developed.

Table 1. Rotational potentials of methyl groups of pure TML and pure TMT as taken from literature [8, 4]. Potentials of TML in TMT can be derived from the measured tunnelling frequencies $\hbar\omega_t$ under the assumptions of either equal shape $\delta = |V_3|/VS$ or equal strength $VS = |V_3| + |V_6|$. k defines the phase relation between V_3 and V_6 (see the text).

System	$\hbar w_t$ [μeV]	Multiplicity	VS [meV]	δ	k
TML	30.8	3	22	0.95	1
pure	74	1	45	0.52	0
TMT	13.2	3	30	0.86	1
pure	1.8	1	49	0.77	1
TML	22	3	25	0.95	1
in TMT	40	1	63	0.52	0
TML	22	3	22	–	1
in TMT	40	1	45	0.63	0

In agreement with this view the dominant tunnelling peak of the more globular TMT molecule at $\hbar\omega_t = 13.2$ μeV shows little shift with increasing concentration of TML. The weak reduction around $c_{Pb} = 0.5$ might be due to local lattice compression around the larger TML defects while the increase at $c_{Pb} > 0.5$ could be the result of an increased free volume for TMT molecules in the TML matrix. According to these simple arguments $\hbar\omega_t$ should increase above 13.2 μeV. It might be that local relaxation of the TML matrix toward the TMT defect stops this shift.

At small concentration of TML two weak additional tunnelling lines are observed at energy transfers 4.8 and 7.8 μeV beside of a weakened tunnel transition at 2.0 μeV. Arguing in the single particle model we could attribute these transitions to the methyl groups of TMT oriented along the threefold molecular axis. At first, these transitions are the only narrow lines in the spectrum. Furthermore the integrated intensity of the three narrow lines is about 1/3 of the broad peak at 13.2 μeV as expected from the occurrence probability of this site. The single particle rotational potential could well depend on the type of the neighboring

molecule [12]. The intensities of the respective sublines then must be given by the occurrence probabilities of the respective environments. In the present case the methyl group under consideration has three equivalent nearest neighbors for symmetry reasons which might be TMT or TML. If lattice sites are occupied statistically the probability of having n TML neighbours is given by a binomial distribution. For $c = 0.1\,(0.2)$ we get $p(0) = 0.73\,(0.51)$, $p(1) = 0.24\,(0.38)$ and $p(2) = 0.03\,(0.10)$. It is obvious that the line intensities do not follow these numbers at least for $c = 0.1$. For further discussion see Section 3.5.

3.5. Deviations from the Single Particle Model?

As we have seen various features of the presented spectra are difficult to be explained in the model of single particle excitations:

1) The intensity ratios between TMT and TML line do not scale well with concentration.

2) New unexpected tunnel lines appear. At *low* h-TML concentrations two new sharp transitions are found whose intensities do not fit into a probability model of next neighbour site occupation. At *large* h-TML concentrations, $c = 0.85$, and deuterated TMT a tunnel line survives around tunnelling transition energies of the protonated TMT molecule. The single particle isotope effect should have shifted the d-TMT tunnelling line into the elastic line and additionally the deuterium scattering cross section would hide it under the strong h-TML lines. Thus the origine of this line is not clear.

For reasons of the molecular geometry our system looks dedicated to show effects of coupled quantum rotors. The only available model which considers an infinite system of coupled tunnel rotors is that of a linear chain [15]. There are various problems with applying this model:

1) The coupling in our system is more complex than in a linear chain. It might be, however, that the linear chain model contains already essential features of coupling.

2) The theory is not approved from first principles.

3) The theory does not yield line intensities so far.

The mathematical expression of this model is a sine-Gordon equation with travelling breather and in- and out-of-phase tunnelling modes as elementary excitations [15]. The theory alllows for an infinite number of excitations and could thus explain the appearance of new transitions. Formally it might be possible to describe the new bands as the ground and excited states of the travelling breather. Recent exact calculations of the levels of up to four coupled tunnel rotors have shown, however, that a large number of interacting neighbours modifies the spectrum of the uncoupled rotor only by rescaling its single particle tunnel splitting [16]. In agreement with this result the tunnelling spectra of the pure systems could be fully and consistently described with the single particle model [4, 8]. The perturbation of the environment in the mixed system was expected to give new insight into intermolecular coupling like in earlier examples, e.g. [9], and to discern in the controversy between single particle and sine-Gordon description. The present state of knowledge, however, does not allow such a conclusion. At first, our experiments were taken with different energy resolution at different spectral ranges and thus do not contain the complete information. Secondly, deuterated TML was not available to get separate spectra from the two components. This would allow a unique assignment between tunnel peaks and methyl groups, especially with respect to new lines. Excluding coupling effects the spectra of the fully protonated sample should come out as the sum of the spectra of the two partially deuterated systems. This could not be proved with the available samples. Finally, the possibility of structural changes has to be definitely ruled out which could also be the source of new features.

4. Summary

Mixed tetramethyltin TMT and -lead TML forms an interesting system of coupled tunnelling rotors. The global changes of the spectra with sample composition can still be described in a single particle model. The strong matrix effect observed for TML in TMT is assigned to both, an increase of the rotational potentials due to closer approach of the methyl groups of neighbouring molecules and a change of potential symmetry toward that in TMT with a weaker sixfold potential term. The tunnel splitting of methyl groups of TMT are little influenced by neighbouring TML molecules. Additional sharp tunnelling lines appearing at low concentration of TML are not fully understood actually but might be assigned to methyl-methyl coupling.

While the pure systems studied originally [4, 8] yielded unambiguous clean results, the interpretation

of the presented data is not straightforward. The more delicate questions asked actually in the field of rotational tunnelling – e.g. single particle vs. collective quantum rotation – require more complex samples. Naturally the tunnel spectra are more complex. To reduce the uncertainty of different explanations, samples have to be characterized structurally, and systematic studies on sequences of well choosen systems are required. This involves often complex chemistry including deuteration. While having yielded new insight, the actual experiments have also raised new questions. Thus, after more than a decade of tunnelling spectroscopy with tetramethyl metal compounds there are still interesting and new questions which can be especially well studied with this unique system of coupled rotors.

Acknowledgement

We thank the ILL for having given beamtime for the proposal and H. Büttner, G. Kearley, and J. Cook for the help with the experiment.

[1] W. Müller-Warmuth, K. H. Duprée, and M Prager, Z. Naturforsch. **39a,** 66 (1984).
[2] G. W. Smith, J. Chem. Phys. **42,** 4229 (1965).
[3] Da Zhang, Thesis, Darmstadt 1990.
[4] M. Prager, K. H. Duprée, and W. Müller-Warmuth, Z. Phys. **B 51,** 309 (1983).
[5] M. Prager and W. Langel, J. Chem. Phys. **88,** 7995 (1988).
[6] B. Krebs, G. Henkel, and M. Dartmann, Acta Cryst. **C 45,** 1010 (1990).
[7] R. Delaplane and M. Prager, ISIS Annual Report RB2353, A 9 (1992).
[8] M. Prager, W. Müller-Warmuth, and K. H. Duprée, Z. Naturforsch. **39a,** 1187 (1984).
[9] Da Zhang, M. Prager, and A. Weiss, J. Chem. Phys. **94,** 1765 (1990).
[10] M. Prager, Da Zhang, and A. Weiss, Physica **B 180 & 181,** 671 (1992).
[11] J. C. Cook, W. Petry, A. Heidemann, and J.-F. Barthelemy, Nucl. Instrum. Meth. **A 312,** 553 (1992).
[12] M. Prager, B. Asmussen, W. Langel, C. J. Charlile, and H. Blank, J. Chem. Phys. **99,** 2052 (1993).
[13] M. Prager and W. Press, J. Chem. Phys. **92,** 5517 (1990).
[14] W. Press, Single Particle Rotations in Molecular Crystals, Springer tracts in modern physica, Vol. 92, Springer, Berlin 1981.
[15] F. Fillaux and C. J. Carlile, Phys. Rev. **B 42,** 5990 (1990).
[16] G. Voll, Z. Phys. **B 90,** 455 (1993).
[17] A. Heidemann, K. J. Lushington, J. A. Morrison, K. Neumaier, and W. Press, J. Chem. Phys. **81,** 5799 (1984).